Check for updates

Received: 29 May 2024 | Revised: 21 June 2024 | Accepted: 24 June 2024

DOI: 10.1002/ardp.202400430

FULL PAPER

ARCH PHARM DPhG
Archiv der Pharmazie

Hydrazinated geraniol derivatives as potential broad-spectrum antiprotozoal agents

Joelien Jooste[1] | Lesetja J. Legoabe[1] | Kayhan Ilbeigi[2] | Guy Caljon[2] | Richard M. Beteck[1]

[1]Centre of Excellence for Pharmaceutical Sciences, North-West University, Potchefstroom, South Africa

[2]Laboratory of Microbiology, Parasitology and Hygiene (LMPH), Infla-Med Centre of Excellence, University of Antwerp, Antwerp, Belgium

Correspondence
Richard M. Beteck, Centre of Excellence for Pharmaceutical Sciences, North-West University, Private Bag X6001, Potchefstroom 2520, South Africa.
Email: 25159194@nwu.ac.za and richmbi1@yahoo.com

Funding information
South African Medical Research Council

Abstract

Geraniol, a primary component of several essential oils, has been associated with broad-spectrum antiprotozoal activities, although moderate to weak. This study primarily concentrated on the synthesis of hydrazinated geraniol derivatives as potential antiprotozoal agents. The synthesised compounds were tested in vitro against different parasitic protozoans of clinical relevance, including *Trypanosoma brucei brucei*, *Trypanosoma brucei rhodesiense*, *Trypanosoma cruzi* and *Leishmania infantum*. Compounds **6**, **8**, **13**, **14** and **15** demonstrated low micromolar activity against the different parasites. Compounds **8**, **13**, **14** and **15** had the highest efficacy against *Trypanosoma brucei rhodesiense*, as indicated by their respective IC_{50} values of 0.74, 0.56, 1.26 and 1.00 µM. Compounds **6**, **14** and **15** displayed the best activity against *Trypanosoma brucei brucei*, with IC_{50} values of 1.49, 1.48 and 1.85 µM, respectively. The activity of compounds **6**, **14** and **15** also extended to intracellular *Trypanosoma cruzi*, with IC_{50} values of 5.14, 6.30 and 4.90 µM, respectively. Compound **6**, with an IC_{50} value of 11.73 µM, and compound **14**, with an IC_{50} value of 8.14 µM, demonstrated some modest antileishmanial activity.

KEYWORDS

geraniol, *Leishmania* infantum, *Trypanosoma brucei brucei*, *Trypanosoma brucei rhodesiense*, *Trypanosoma cruzi*

1 | INTRODUCTION

Human African trypanosomiasis (HAT), commonly known as sleeping sickness, is mainly caused by the protozoa *Trypanosoma brucei gambiense* in West and Central Africa.[1–3] This parasite accounts for 92% of all chronic HAT infections due to its prevalence in 24 West and Central African countries.[1] However, in 13 East and Southern African countries, the disease is primarily caused by *Trypanosoma brucei rhodesiense*, which mainly affects cattle and wildlife but accounts for 8% of human cases.[1–4]

Infections by *T. b. gambiense* often require several years to develop into a typical disease with central nervous system (CNS) involvement, whereas *T. b. rhodesiense* induces an acute infection that can result in mortality within a matter of weeks to months.[2] Both subspecies of *T. brucei* are transmitted by tsetse flies belonging to the *Glossina* genus.[5] *T. b. gambiense* is a primary target in the latest campaigns against HAT as it involves human-to-human transmission.[5]

When injected into the bloodstream, these parasites cause a stage I infection, in which the parasites are replicating primarily in the

This is an open access article under the terms of the Creative Commons Attribution-NonCommercial-NoDerivs License, which permits use and distribution in any medium, provided the original work is properly cited, the use is non-commercial and no modifications or adaptations are made.
© 2024 The Author(s). *Archiv der Pharmazie* published by Wiley-VCH GmbH on behalf of Deutsche Pharmazeutische Gesellschaft.

blood and lymph.[2] From blood and lymph, the parasites spread to different organs, such as the CNS.[2] Upon crossing the blood–brain barrier and entry into the nervous system, stage II of the disease is ushered in, and most symptoms are observed.[2,4]

The symptoms in the first stage appear 1–3 weeks after the bite of the tsetse fly, and they include a local skin reaction (inoculation chancre), headache, malaise, joint pain, weight loss, enlarged lymph nodes, fatigue, fever and a rash.[4,6,7] The symptoms of the second stage are more evident and include symptoms such as weakness, tremors, speech abnormalities, ataxia, behaviour changes, seizures and confusion.[4,7] The disturbance of a person's sleep cycle is why the disease got its name.[4] If the infection in stage II is not effectively treated, it leads to a coma and death.[8]

The current treatment options for *T. b. gambiense* include intramuscular pentamidine injection (Figure 1) during the first stage.[4,9] Intravenous eflornithine (Figure 1) is used as monotherapy in the first stage of infection.[4,9] The combination therapy of intravenous eflornithine and oral nifurtimox is known as the Nifurtimox and Eflornithine Combination Therapy (NECT) for *T. b. gambiense* in the second stage.[4,9] Oral fexinidazole (Figure 1) is also available for the first and nonsevere second stage.[4,9]

The current treatment for *T. b. rhodesiense* involves intravenous suramin during the first stage, which might lead to adverse effects such as nephrotoxicity and thrombocytopenia.[4,7,9] To treat the second stage, toxic melarsoprol is administered intravenously.[4,7,9] The toxicity of melarsoprol is attributed to its composition as an arsenic derivative, which can lead to the development of severe encephalopathy syndrome that is associated with a fatality rate of 5%.[7,9] The drugs mentioned above have been used for decades, except for fexinidazole.[10] The World Health Organisation (WHO) released new guidelines for fexinidazole with precautions and restrictions on use by patients older than 6 years or with a body weight of more than 20 kg and under the supervision of trained medical staff.[4]

American trypanosomiasis, or Chagas disease, is a parasitic disease caused by *Trypanosoma cruzi*, and 6–7 million people worldwide are infected with this parasite.[11] It is transmitted to humans and animals through triatomine bugs, also known as kissing bugs.[11] Chagas disease has two stages: the acute stage, which lasts 4–6 weeks, and the chronic stage, which lasts years.[11,12] Symptoms such as fever, headache, swollen lymph glands, muscle aches, abdominal pain and chest pain can occur in the acute stage.[11] During the chronic stage, parasites can be found in the heart muscle and digestive system. They can cause lesions in the nervous system and heart muscle, which can lead to cardiovascular problems like arrhythmias, progressive heart failure, myocarditis and even death.[11,12]

The current treatment for Chagas disease has been used for more than 40 years.[13] It involves nifurtimox and benznidazole.[13] These two drugs are not ideal as *T. cruzi* developed resistance over the years to these drugs, and these drugs have severe adverse effects like convulsions, vertigo, insomnia, depression, anorexia, nausea and vomiting.[14]

More than 20 *Leishmania* species can cause human leishmaniasis[15] and are spread by the female phlebotomine sand fly.[16] *Leishmania* infections exhibit a broad diversity and can be classified into three clinical forms: (i) visceral leishmaniasis, a lethal form if left untreated, (ii) mucocutaneous leishmaniasis, a severe disfiguring infection of the skin and mucosa and (iii) cutaneous leishmaniasis, the most common form causing skin lesions that are mostly self-limiting.[15] Human visceral leishmaniasis is caused by *Leishmania donovani* and *Leishmania infantum*.[17] While *L. donovani* is transmitted anthropologically, dogs are the main reservoir for the visceral *L. infantum*, and humans are the accidental host.[16,17] The incubation period can range from a minimum of 2–6 months, but it can extend to several years.[15] The beginning of symptoms is characterised by a gradual increase in fever, loss of weight and abdominal pain.[15] In a chronic infection, enlargement of the spleen is noted.[16]

For the treatment of visceral leishmaniasis, miltefosine was developed as an oral medication in 2003,[15] but proved to be teratogenic and associated with gastrointestinal side effects and ocular toxicity.[18,19] Intravenous liposomal amphotericin B (L-AmB) was introduced after amphotericin B deoxycholate, showing higher efficacy and lower toxicity.[20]

Despite advancements in the treatment of these diseases, several challenges persist, including limited therapeutic options, toxicity, drug resistance, poor pharmacological effectiveness and the occurrence of severe adverse effects.[13,21] These require the development of novel drugs.[13,20,21]

Terpenoids are one of the largest and most diverse classes of natural compounds, with over 70,000 different chemical structures.[22] They are valuable in various industries, such as pharmaceuticals, agriculture, flavouring, fragrances and cosmetics.[23]

Geraniol (GN) is an aliphatic monoterpenoid alcohol found in various flower species and is distinguished by its aromatic, rose-like scent.[24,25] Different pharmacological activities of GN are reported in the literature.[25] These include anti-inflammatory activity,[26] antiepileptic activity,[27] anti-neurogenerative activity,[28] antiviral activity against Herpes Simplex Virus type 1,[29] antibacterial activity against *Streptococcus pneumonia*[30] and antiparasitic activity,[31] anticancer activity,[32] antidiabetic activity.[33]

GN derivatives have been found to exhibit inhibitory effects against fungi [34] and human enzymes.[35] The ester derivative of GN (**GN1**) demonstrated a specific inhibitory activity on human carboxylesterase 2 (hCES2) with minimal toxicity, suggesting its potential as an inhibitor.[35] In a study by Chaves et al.,[34] a series of geranylated phenols (**GN2–6**; Figure 2) were tested against the mycelial growth of *Phytophthora cinnamomic*. The study found that the geranylated phenols were as effective as Metalaxil, a common fungicide.[34]

Several studies have reported different pharmacological activity of hydrazides. These activities include anticonvulsants,[36] antidepressant,[37] anti-inflammatory,[38] antimicrobial,[39] antimycobacterial,[40] antitumoral,[41] vasodilator,[42] antifungal,[43] antiviral[44]

15214184, 2024, 10, Downloaded from https://onlinelibrary.wiley.com/doi/10.1002/ardp.202400430 by North-West University, Wiley Online Library on [05/01/2026]. See the Terms and Conditions (https://onlinelibrary.wiley.com/terms-and-conditions) on Wiley Online Library for rules of use; OA articles are governed by the applicable Creative Commons License

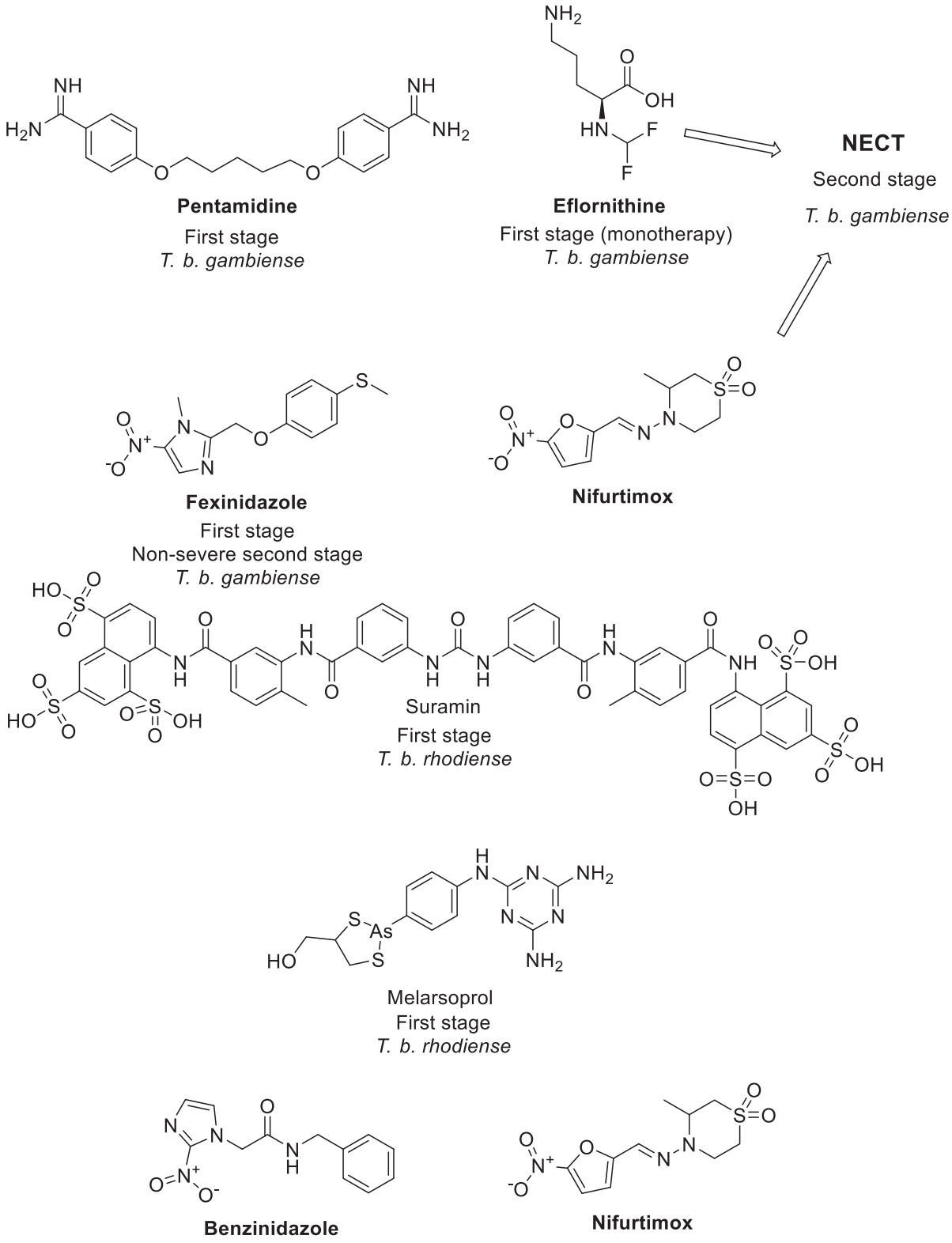

FIGURE 1 Structures of anti-trypanosoma and anti-leishmanial drugs.

and antiparasitic.[45] Hydrazide functional group is composed of azomethine and acyl moieties.[46] Hydrazides can decrease leucocyte migration, block the Nuclear factor kappa B (NF-kB) enzyme, and ultimately hinder the production of reactive oxygen species (ROS).[47]

This study aims to synthesise GN derivatives bearing hydrazide and to investigate their potential antiprotozoal activity. The compounds were screened against various parasites, including *T. cruzi*, *T. b. brucei*, *T. b. rhodesiense* and *L. infantum*. The screening results revealed promising broad-spectrum antiprotozoal activities.

15214184, 2024, 10, Downloaded from https://onlinelibrary.wiley.com/doi/10.1002/ardp.202400430 by North-West University, Wiley Online Library on [05/01/2026]. See the Terms and Conditions (https://onlinelibrary.wiley.com/terms-and-conditions) on Wiley Online Library for rules of use; OA articles are governed by the applicable Creative Commons License

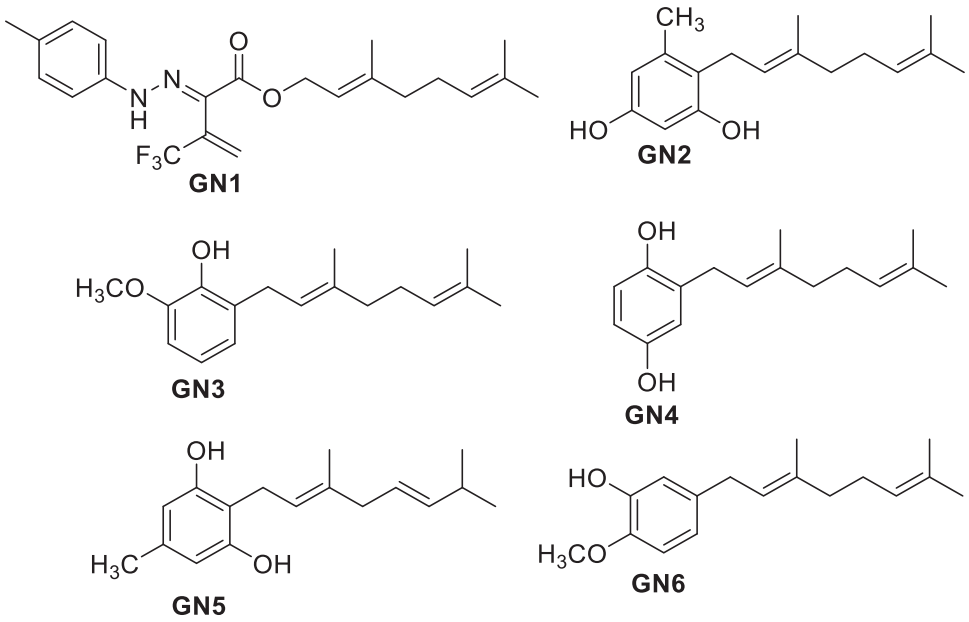

FIGURE 2 Examples of some geranylated compounds exhibiting biological activities.

2 | RESULTS AND DISCUSSION

2.1 | Chemistry

The target compounds **1–15** were synthesised following the processes outlined in Scheme 1. Geranyl bromide was subjected to nucleophilic substitution (SN_2 substitution) with ethyl paraben to form intermediate **a**, an ether. The hydrazinolysis[48] of **a** with hydrazine hydrate resulted in intermediate **b**, a hydrazide. Intermediate **b** underwent a Schiff base condensation reaction with various aldehydes in the presence of catalytic amounts of acetic acid, resulting in the formation of compounds **1–15** with yields ranging from 17.1% to 62.1%.

The target compounds' structures were confirmed with proton and carbon nuclear magnetic resonance (NMR). The appearance and absence of specific peaks were used to verify successful chemical transformation. The appearance of a doublet at 4.63 ppm, a quartet at 4.27 ppm, and a multiplet at 1.30 ppm on the proton NMR of intermediate **a** implies that the ether formed. The absence of a quartet at 4.27 ppm and multiplet at 1.30 ppm on the proton NMR of intermediate **b**, with the addition of a doublet at 4.60 ppm and a singlet at 9.58 ppm on the proton NMR and the absence of a peak around 60 ppm on the carbon NMR, implies that intermediate **b** formed a hydrazide. For compounds **1–14**, the singlet peaks at approximately 11 and 9 ppm and the absence of a singlet peak at 9.5 ppm and a triplet peak at 2.1 ppm on the proton NMR indicates that the Schiff base formed in all the compounds. Due to the low solubility of some compounds in Acetone-d_6, all the carbon peaks were not visible. High-resolution mass spectrometry (HRMS) was used to verify each compound's molecular mass.

2.2 | Antiprotozoal activity and cytotoxicity evaluation

The compounds underwent in vitro testing to determine their antitrypanosomal and antileishmanial action against the parasites *T. cruzi*, *T. brucei brucei*, *T. b. rhodesiense* and *L. infantum*. The toxicity of each compound was assessed using MRC-5_{SV2} (human foetal lung fibroblast) cells and primary mouse macrophages (PMM).

Table 1 summarises the antiparasitic and cell toxicity of compounds **1–15**. Several compounds showed broad-spectrum antiprotozoal activities. However, some compounds also exhibited cytotoxicity towards the MRC-5_{SV2} human fibroblasts and PMM.

Analysis of compounds **1–3** shows that the position of the nitro group determines in part their potency against *T. b. rhodesiense*. Compound **2** (IC_{50} 1.79 ± 0.32 μM), with the nitro group in the *meta* position, has more potent activity against *T. b. rhodesiense* than the other two compounds, where compound **1** (IC_{50} 9.51 μM) has the nitro group in the *ortho* position and compound **3** (IC_{50} 5.54 ± 3.19 μM) has the nitro group in the *para* position. Comparing the potency of compounds **1–3** against *T. b. brucei*, significantly lower activity was recorded in general with IC_{50} values >10 μM. No discernible activity against *L. infantum* was recorded.

Compounds **4** and **5** contain a fluoro functional group. Compound **5** has slightly higher antiprotozoal activity compared with compound **4**, especially against *T. b. rhodesiense*, with IC_{50} values of 1.93 versus 11.10 μM against *T. b. rhodesiense*, 23.00 versus 43.92 μM against *T. b. brucei*, and 21.81 versus 45.58 μM against *L. infantum*, respectively. The higher activity of compound **5** is linked to the fluoro group in a *para* position, whereas compound **4** has the fluoro group in a *meta* position.

15214184, 2024, 10, Downloaded from https://onlinelibrary.wiley.com/doi/10.1002/ardp.202400430 by North-West University, Wiley Online Library on [05/01/2026]. See the Terms and Conditions (https://onlinelibrary.wiley.com/terms-and-conditions) on Wiley Online Library for rules of use; OA articles are governed by the applicable Creative Commons License

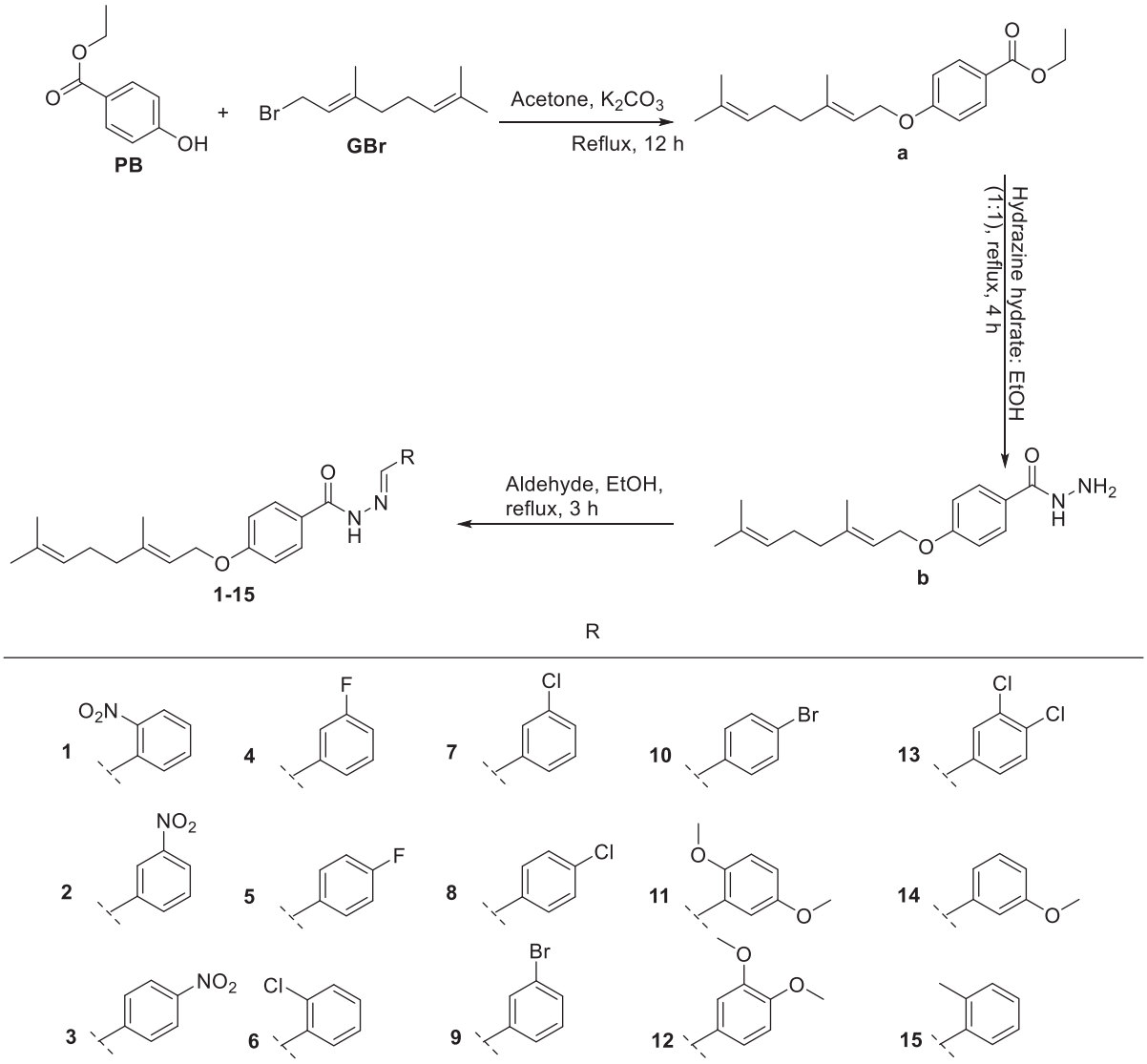

SCHEME 1 Synthesis of target compounds **1–15**.

Compounds **6–8** all have a chloro functional group and display potent activity against trypanosomes. Compound **8** (IC_{50} 0.74 ± 0.11 μM) with the chloro in the *para* position has the highest *T. b. rhodesiense* activity, followed by compound **7** (IC_{50} 1.73 ± 0.12 μM) with the chloro in the *meta* position and then compound **6** (IC_{50} 1.99 ± 0.01 μM) with chloro in the *ortho* position. Compound **6** (IC_{50} 1.49 ± 0.46 μM) has the highest activity against *T. b. brucei*, followed by compound **8** (IC_{50} 12.95 ± 11.65 μM) and compound **7** (IC_{50} 32.62 ± 31.38 μM). Compound **6** displays activity against *T. cruzi* with an IC_{50} value of 5.14 ± 2.55 μM, while compounds **7** and **8** are inactive against this target species. Against *L. infantum*, only very modest activity was recorded, with compound **6** (IC_{50} 11.73 ± 1.37 μM) being slightly more potent than compound **7** (IC_{50} 28.70 ± 3.30 μM) and compound **8** (IC_{50} 36.71 ± 14.08 μM). Overall, compound **6**, bearing chloro functional group, is the most potent and broad spectrum anti-protozoal compound in this series.

Compounds **9** and **10** contain a bromo functional group. Both show some activity against *T. b. rhodesiense* (**9**: IC_{50} 5.14 μM; **10:** IC_{50} 4.67 ± 3.33 μM) but are largely inactive against *T. b. brucei*, *T. cruzi* and *L. infantum*. Compounds **11** and **12** contain two methoxy groups, rendering the compounds largely inactive against any of the tested parasites.

In summary, compounds with the best activity against *T. b. rhodesiense* were *meta* or *para* substituted, and they are **8** (IC_{50} 0.74 ±;0.11 μM), **13** (IC_{50} 0.56 ± 0.17 μM), **14** (IC_{50} 1.26 ± 0.80 μM) and **15** (IC_{50} 1.00 ± 0.45 μM). The compounds with the best activity against *T. b. brucei* were *ortho* or *meta* substituted; **6** (IC_{50} 1.49 ± 0.46 μM), **14** (IC_{50} 1.48 ± 0.30 μM) and **15** (IC_{50} 1.85 ± 1.31 μM). For *L. infantum*, the compounds with the best activity were compound **6** (IC_{50} 11.73 ± 1.37 μM) and compound **14** (IC_{50} 8.14 ± 0.90 μM). The best activity against *T. cruzi* was recorded for compounds substituted at *ortho* and *meta*-positions, like **6** (IC_{50} 5.14 ± 2.55 μM), **14** (IC_{50} 6.30 ± 1.24 μM) and **15** (IC_{50} 4.90 ± 3.16 μM). Although compound **14** showed broad-spectrum antiprotozoal activity, it also exhibited MRC-5_{SV2} cytotoxicity with a CC_{50} value of 11.21 ± 6.94 μM.

15214184, 2024, 10, Downloaded from https://onlinelibrary.wiley.com/doi/10.1002/ardp.202400430 by North-West University, Wiley Online Library on [05/01/2026]. See the Terms and Conditions (https://onlinelibrary.wiley.com/terms-and-conditions) on Wiley Online Library for rules of use; OA articles are governed by the applicable Creative Commons License

TABLE 1 Target compound structures with corresponding antiprotozoal activity and cytotoxicity.

Name	Structure	MRC-5_{SV2} CC_{50}(μM)	*Leishmania infantum* IC_{50}(μM)	*Trypanosoma cruzi* IC_{50}(μM)	*Trypanosoma brucei* IC_{50}(μM)	*Trypanosoma brucei rhodesiense* IC_{50}(μM)	PMM cytotoxicity CC_{50}(μM)
1	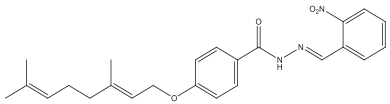	>64.00	>64.00	>64.00	39.61	9.51	>64.00
2	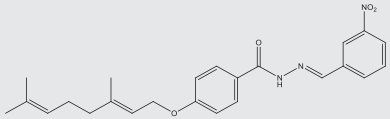	>64.00	48.23 ± 15.77	>64.00	>64.00	1.79 ± 0.32	48.00 ± 16
3	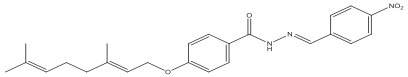	>64.00	>64.00	>64.00	17.04 ± 13.04	5.54 ± 3.19	>64.00
4	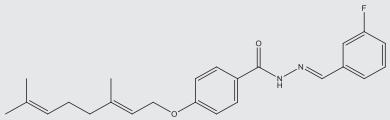	>64.00	45.58	>64.00	43.92	11.10	45.25
5	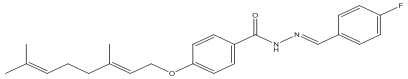	>64.00	21.81 ± 10.19	>64.00	23.00 ± 13.49	1.93 ± 0.24	>64.00
6	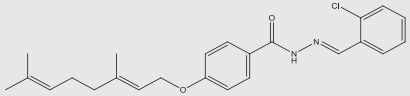	>64.00	11.73 ± 1.37	5.14 ± 2.55	1.49 ± 0.46	1.99 ± 0.01	>64.00
7	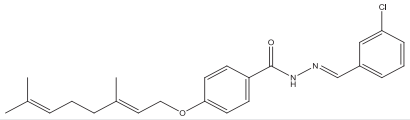	>64.00	28.70 ± 3.30	>64.00	32.62 ± 31.38	1.73 ± 0.12	>64.00
8	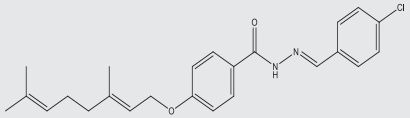	>64.00	36.71 ± 14.08	>64.00	12.95 ± 11.65	0.74 ± 0.11	>64.00
9	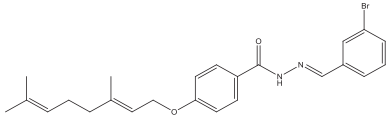	>64.00	36.76	>64.00	30.62	5.14	>64.00
10	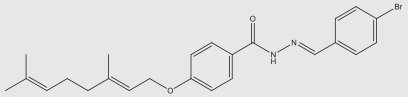	>64.00	17.66 ± 4.96	>64.00	33.26 ± 30.74	4.67 ± 3.33	48.00 ± 16

15214184, 2024, 10, Downloaded from https://onlinelibrary.wiley.com/doi/10.1002/ardp.202400430 by North-West University, Wiley Online Library on [05/01/2026]. See the Terms and Conditions (https://onlinelibrary.wiley.com/terms-and-conditions) on Wiley Online Library for rules of use; OA articles are governed by the applicable Creative Commons License

TABLE 1 (Continued)

Name	Structure	MRC-5_{SV2} CC_{50}(μM)	*Leishmania infantum* IC_{50}(μM)	*Trypanosoma cruzi* IC_{50}(μM)	*Trypanosoma brucei* IC_{50}(μM)	*Trypanosoma brucei rhodesiense* IC_{50}(μM)	PMM cytotoxicity CC_{50}(μM)
11	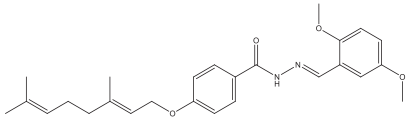	>64.00	>64.00	>64.00	37.51 ± 26.49	16.20 ± 14.73	>64.00
12	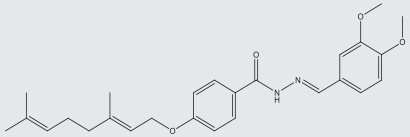	>64.00	15.41 ± 6.37	>64.00	>64.00	32.96 ± 31.04	48.00 ± 16
13	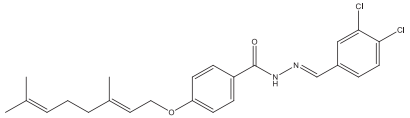	>64.00	>64.00	>64.00	>64.00	0.56 ± 0.17	>64.00
14	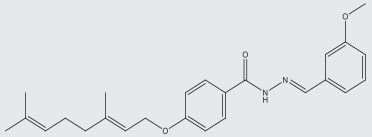	11.21 ± 6.94	8.14 ± 0.90	6.30 ± 1.24	1.48 ± 0.30	1.26 ± 0.80	>64.00
15	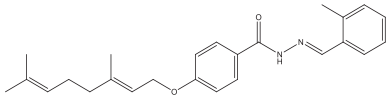	33.36 ± 24.17	20.08 ± 13.11	4.90 ± 3.16	1.85 ± 1.31	1.00 ± 0.45	>64.00
MF	-	-	7				
Sura	-	-	-	-	0.04	0.05	-
Benz	-	-	-	1.3	-	-	-
Tam	-	10	-	-	-	-	-
GN[49,50]		-	24	-	95	-	-

Abbreviations: Benz, benznidazole; GN, geraniol; MF, miltefosine; Sura, suramin; Tam, tamoxifen.

15214184, 2024, 10, Downloaded from https://onlinelibrary.wiley.com/doi/10.1002/ardp.202400430 by North-West University, Wiley Online Library on [05/01/2026]. See the Terms and Conditions (https://onlinelibrary.wiley.com/terms-and-conditions) on Wiley Online Library for rules of use; OA articles are governed by the applicable Creative Commons License

2.3 | Absorption, distribution, metabolism and excretion (ADME) analysis of compound 6 with SwissADME

We used the SwissADME tool (www.swissadme.ch, accessed on June 18, 2024) to predict the drug-likeness of the most promising compound, compound **6**. The property radar shows six drug-likeness properties (Figure 3): size, lipophilicity, polarity, solubility, flexibility and saturation. On this radar, the pink middle represents the physiochemical range for a drug with excellent oral bioavailability. Compound **6** showed fair saturation with a fraction Csp3 < 0.25 and a good size with a molecular weight < 500 g/mol. The compound is, however, poorly water-soluble with Log S < −6, but has a favourable polarity with TPSA<140 Å². Its favourable polarity suggests a positive impact on gastrointestinal absorption. Compound **6** complies with all the Lipinski rules, except that its MLOGP is greater than 4.15. The lipophilicity of compound **6** is greater than 5 (XLOGP3 = 7.68), which predicts that the compound will have a low solubility and poor oral absorption and high metabolic turnover. Compound **6** is not a pan assay interfering compound, which is consistent with the results of the experimental data that showed it doesn't affect human cell lines.

3 | CONCLUSION

We have effectively synthesised novel GN derivatives. The antiprotozoal activity of the substances was assessed by a battery of in vitro tests. Several compounds exhibited antiprotozoal activity with IC_{50} values of < 10 µM. Compounds **8**, **13**, **14** and **15** were most potent against *T. b. rhodesiense*, as evidenced by their respective IC_{50} values of 0.74, 0.56, 1.26 and 1.00 µM. Compounds **6**, **14** and **15** had the highest efficacy against *T. b. brucei* with respective IC_{50} values of 1.49, 1.48 and 1.85 µM. Compound **15** showed the highest activity level against *T. cruzi* (IC_{50} 4.90 µM). Compounds **6** (IC_{50} 11.73 µM) and **14** (IC_{50} 8.14 µM) exhibited some modest antileishmanial activity. Noteworthy, compound **6** shows antiprotozoal activity across the four parasite species included in the tests and proved to be nontoxic against a human fibroblast cell line and PMM. In comparison with the reported antiparasitic activities for GN, this compound is more potent and selective. In conclusion, we have observed that the derivatization of GN results in novel substances with broad-spectrum antiprotozoal activities that are worth exploring further.

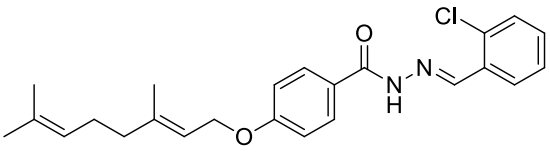

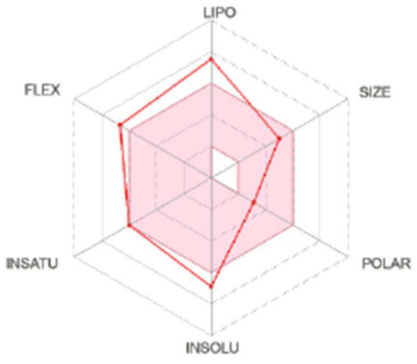

Property radar

Drug likeness properties

- **Lipophilicity:** XLOGP3 = 7.68
- **Molecular weight:** 410.94 g/mol
- **Number of rotatable bonds:** 10
- **Number of H-bond acceptors:** 3
- **Number of H-bond donors:** 1
- **Polarity:** TPSA = 50.69 Å²
- **Solubility:** Log *S* = -6.87
- **Saturation:** Fraction Csp^3 = 0.25
- **Skin permeation:** Log K_p = -3.35 cm/s
- **Bioavailability:** 0.55
- **BBB permeation:** No
- **GI absorbance:** Yes
- **CYP1A2 inhibitor:** Yes
- **CYP2C19 inhibitor:** No
- **CYP2C9 inhibitor:** Yes
- **CYP2D6 inhibitor:** No
- **CYP3A4 inhibitor:** Yes

FIGURE 3 Absorption, distribution, metabolism and excretion (ADME) analysis of compound **6** with Swiss-ADME.

15214184, 2024, 10, Downloaded from https://onlinelibrary.wiley.com/doi/10.1002/ardp.202400430 by North-West University, Wiley Online Library on [05/01/2026]. See the Terms and Conditions (https://onlinelibrary.wiley.com/terms-and-conditions) on Wiley Online Library for rules of use; OA articles are governed by the applicable Creative Commons License

4 | MATERIALS AND METHODS

4.1 | Chemistry

4.1.1 | Chemicals and general methods

The reagents and solvents used in this study were obtained from different chemical suppliers such as Sigma-Aldrich, Ace, Rochelle and Ambeed, and they were used in their original form without any purification. The progress of each reaction was monitored with thin layer chromatography (TLC) using Merck $60F_{254}$ silica gel plates supported on aluminium sheets (0.20 mm thickness). The TLC plates were examined using ultraviolet light. Proton (^{1}H) and Carbon-13 (^{13}C) NMR spectra (see the Supporting Information) were recorded on a Bruker Avance III 600 spectrophotometer at 600 and 150 MHz, respectively. MestReNova software, version 14.1.2, was used to analyse the NMR data. Chemical shifts (δ) were reported in parts per million (ppm) and relative to deuterated acetone (acetone-d_6) or deuterated dimethylsulphoxide (DMSO-d_6). The chemical shifts of acetone-d_6 and DMSO-d_6 for the ^{1}H-NMR are 2.05 and 2.5 ppm, respectively. The chemical shifts for the ^{13}C-NMR of acetone-d_6 and DMSO-d_6 are 29.8, 206.03 and 39.5 ppm, respectively. All coupling constants (J) were reported in Hz and are abbreviated as follows: s (singlet), d (doublet), dd (doublet of doublet), t (triplet) and m (multiplet). Using the Büchi B-545 instrument, melting points (mp) were obtained. A Bruker microOTOF-Q II mass spectrometer was used to record the high-resolution mass spectra (HRMS) utilising atmospheric pressure chemical ionisation (APCI) in positive ion mode.

The InChI codes of the investigated compounds, together with some biological activity data, are provided as Supporting Information.

4.1.2 | Synthesis of compound a (intermediate a)

A round-bottom flask was charged with 1 g of ethyl paraben (6.02 mmole), 2.4 mL of geranyl bromide (2 equivalents), potassium carbonate (2.5 g, 18.1 mmole, 3 equivalents), 20 mL of acetone as the solvent and the mixture was refluxed for 12 h. After completion of the reaction as indicated by TLC, a rotary evaporator was used to evaporate the remaining acetone. Water, 50 mL, was added, followed by extraction with ethyl acetate (20 mL × 3). The combined ethyl acetate fractions were evaporated to dryness using a rotary evaporator to afford intermediate **a** (1.6 g, 5.4 mmole, 90%).

4.1.3 | Synthesis of compound b (intermediate b)

Intermediate **a** (1 g, 3.3 mmole) was refluxed for 4 h in a round-bottom flask containing a 1:1 ratio of ethanol to hydrazine hydrate. After reaction completion as indicated by TLC monitoring, the mixture was concentrated using a rotary evaporator. Ice water was added, and the resultant precipitate was filtered and dried overnight to provide intermediate **b** (0.76 g, 2.6 mmole, 80%).

4.1.4 | Synthesis of compounds 1–15

In a round-bottom flask, 0.2 g (0.693 mmole) of intermediate **b**, one equivalent of the appropriate aldehyde, 10 mL of ethanol and 10 drops of acetic acid as catalyst were added and refluxed for 3 h. After completion (confirmed by TLC), ethanol was evaporated, and the resultant crude was washed with 30 mL of deionized water and left to dry overnight. The process resulted in compounds **1**–**15**, with yields ranging between 16.9% and 62.1%.

(*E*)-4-{[(*E*)-3,7-Dimethylocta-2,6-dien-1-yl]oxy}-*N*′-(2-nitrobenzylidene)benzohydrazide (**1**): Off-white powder; 34.2% yield; mp: 123.°C; ^{1}H NMR (600 MHz, Acetone-d_6) δ 11.63 (s, 1H), 9.15 (s, 1H), 8.54 (d, J = 4.8 Hz, 1H), 8.32 (d, J = 6.3 Hz, 1H), 8.27 (dd, J = 2.2, 1.5 Hz, 2H), 8.08 – 8.03 (m, 1H), 7.97–7.91 (m, 1H), 7.32 (dd, J = 8.8, 3.7 Hz, 2H), 5.80–5.74 (m, 1H), 5.42–5.36 (m, 1H), 4.95 (d, J = 6.3 Hz, 2H), 2.42 (d, J = 7.2 Hz, 2H), 2.38 (d, J = 6.9 Hz, 2H), 2.33 (s, 3H), 1.93 (s, 3H), 1.88 (s, 3H). ^{13}C NMR (151 MHz, Acetone-d_6) δ 162.07, 162.04, 148.70, 140.80, 133.33, 131.24, 130.25, 129.60, 129.32, 128.12, 125.36, 124.50, 123.81, 119.59, 119.40, 114.39, 64.88, 39.26, 26.15, 24.91, 16.84, 15.80. HRMS-APCI m/z calcd for $C_{24}H_{28}N_3O_4$ $[M+H]^+$, 422.2074, found 422.2088.

(*E*)-4-{[(*E*)-3,7-Dimethylocta-2,6-dien-1-yl]oxy}-*N*′-(3-nitrobenzylidene)benzohydrazide (**2**): Off-white powder; 44.7% yield; mp: 125–126°C; ^{1}H NMR (600 MHz, DMSO-d_6) δ ^{1}H NMR (600 MHz, Acetone) δ 11.19 (s, 1H), 8.59 (s, 1H), 8.27 (d, J = 8.2 Hz, 1H), 8.18 (d, J = 7.7 Hz, 1H), 7.99 (dd, J = 8.8, 2.4 Hz, 2H), 7.78–7.74 (m, 1H), 7.75–7.73 (m, 1H), 7.06 (dd, J = 8.8, 2.3 Hz, 2H), 5.53–5.48 (m, 1H), 5.16–5.11 (m, 1H), 4.70 (d, J = 6.5 Hz, 2H), 2.16 (d, J = 7.7 Hz, 2H), 2.12 (d, J = 7.5 Hz, 2H), 1.79 (s, 3H), 1.67 (s, 3H), 1.62 (s, 3H). ^{13}C NMR (151 MHz, Acetone-d_6) δ 162.04, 162.01, 148.80, 140.81, 137.04, 132.77, 131.24, 130.11, 129.56, 125.49, 123.88, 123.81, 121.21, 119.59, 114.38, 64.88, 39.26, 26.15, 24.91, 16.83, 15.80. HRMS-APCI m/z calcd for $C_{24}H_{28}N_3O_4$ $[M+H]^+$, 422.2074, found 422.2088.

(*E*)-4-{[(*E*)-3,7-Dimethylocta-2,6-dien-1-yl]oxy}-*N*′-(4-nitrobenzylidene)benzohydrazide (**3**): Light yellow powder; 17.1% yield; mp: 138°C; ^{1}H NMR (600 MHz, Acetone-d_6) δ 11.24 (s, 1H), 8.62 (s, 1H), 8.31 (d, J = 3.1 Hz, 1H), 8.29 (d, 1H), 8.03 (dd, 1H), 8.02–7.98 (m, 2H), 8.00–7.97 (m, 1H), 7.06 (dd, J = 8.9, 3.0 Hz, 2H), 5.51 (d, J = 6.9 Hz, 1H), 5.14 (d, J = 6.9 Hz, 1H), 4.70 (d, J = 6.5 Hz, 2H), 2.16 (d, J = 7.8 Hz, 2H), 2.12 (d, J = 7.6 Hz, 2H), 1.79 (s, 3H), 1.67 (s, 3H), 1.62 (s, 3H)). ^{13}C NMR (151 MHz, Acetone-d_6) δ 162.06, 162.04, 148.33, 141.28, 140.83, 131.25, 129.53, 127.81, 125.38, 123.84, 123.81, 119.57, 119.37, 114.40, 64.89, 39.26, 26.15, 24.91, 16.84, 15.80. HRMS-APCI m/z calcd for $C_{24}H_{28}N_3O_4$ $[M+H]^+$, 422.2074, found 422.2087.

(*E*)-4-{[(*E*)-3,7-Dimethylocta-2,6-dien-1-yl]oxy}-*N*′-(3-fluorobenzylidene)benzohydrazide (**4**): White powder; 33.7% yield; mp: 95–97°C; ^{1}H NMR (600 MHz, DMSO-d_6) δ 11.05 (s, 1H), 8.51 (s, 1H), 8.01–7.95 (m, 2H), 7.56 (d, J = 8.6 Hz, 2H), 7.51–7.46 (m, 1H), 7.22–7.16 (m, 1H), 7.07–7.02 (m, 2H), 5.53–5.48 (m, 1H), 5.16–5.11 (m, 1H), 4.69 (d, J = 6.3 Hz, 2H), 2.16 (d, J = 6.8 Hz, 2H), 2.12 (d, J = 7.9 Hz, 2H), 1.79 (s, 3H), 1.67 (s, 3H), 1.62 (s, 3H). ^{13}C NMR (151 MHz, Acetone-d_6) δ 163.85, 162.23, 161.91, 140.77, 137.69, 131.24, 130.63, 130.57, 125.66, 123.81, 123.41, 123.39, 119.62, 116.45, 116.31, 114.34,

15214184, 2024, 10, Downloaded from https://onlinelibrary.wiley.com/doi/10.1002/ardp.202400430 by North-West University, Wiley Online Library on [05/01/2026]. See the Terms and Conditions (https://onlinelibrary.wiley.com/terms-and-conditions) on Wiley Online Library for rules of use; OA articles are governed by the applicable Creative Commons License

112.90, 112.75, 64.86, 39.26, 26.15, 24.91, 16.83, 15.79. HRMS-APCI *m/z* calcd for $C_{24}H_{28}FN_2O_2$ $[M+H]^+$, 395.2129, found 395.2141.

(*E*)-4-{[(*E*)-3,7-Dimethylocta-2,6-dien-1-yl]oxy}-*N*′-(4-fluorobenzylidene)benzohydrazide (**5**): White powder; 46.5% yield; mp: 135–136.°C; ^{1}H NMR (600 MHz, Acetone-d_6) δ 10.97 (s, 1H), 8.51 (s, 1H), 7.98 (d, J = 6.8 Hz, 2H), 7.82 (s, 2H), 7.33–7.26 (m, 1H), 7.21 (d, J = 3.2 Hz, 1H), 7.07–7.02 (m, 2H), 5.53–5.48 (m, 1H), 5.15–5.11 (m, 1H), 4.69 (d, J = 5.3 Hz, 2H), 2.16 (d, J = 7.7 Hz, 2H), 2.07 (d, J = 2.0 Hz, 2H), 1.79 (s, 3H), 1.67 (s, 3H), 1.62 (s, 3H). ^{13}C NMR (151 MHz, Acetone-d_6) δ 164.45, 162.81, 161.83, 140.75, 131.56, 131.24, 130.69, 129.17, 129.11, 125.80, 123.81, 119.63, 115.74, 115.67, 115.52, 114.33, 64.85, 39.26, 26.15, 24.91, 16.83, 15.79. HRMS-APCI *m/z* calcd for $C_{24}H_{28}FN_2O_2$ $[M+H]^+$, 395.2129, found 395.2148.

(*E*)-*N*′-(2-Chlorobenzylidene)-4-{[(*E*)-3,7-dimethylocta-2,6-dien-1-yl]oxy}benzohydrazide (**6**): White solid; 46.5% yield; mp: 102°C; ^{1}H NMR (600 MHz, DMSO-d_6) δ 11.94 (s, 1H), 8.87 (s, 1H), 8.05–8.02 (m, 2H), 7.95 (d, J = 9.8 Hz, 2H), 7.54 (d, J = 10.8 Hz, 1H), 7.45 (d, J = 10.2 Hz, 1H), 7.07 (d, J = 10.6 Hz, 2H), 5.48 –5.41 (m, 1H), 5.11–5.05 (m, 1H), 4.65 (d, J = 4.2 Hz, 2H), 2.52 (d, J = 13.2 Hz, 2H), 2.08 (d, J = 11.0 Hz, 2H), 1.73 (s, 3H), 1.64 (s, 3H), 1.59 (s, 3H). ^{13}C NMR (151 MHz, DMSO-d_6) δ 163.06, 161.85, 143.45, 141.19, 133.56, 132.26, 131.77, 130.39, 130.37, 130.03, 128.06, 127.31, 125.52, 124.22, 119.79, 114.87, 65.16, 39.39, 26.29, 25.94, 18.03, 16.86. HRMS-APCI *m/z* calcd for $C_{24}H_{28}ClN_2O_2$ $[M+H]^+$, 411.1834, found 411.1835.

(*E*)-*N*′-(3-Chlorobenzylidene)-4-{[(*E*)-3,7-dimethylocta-2,6-dien-1-yl]oxy}benzohydrazide (**7**): White solid; 32.3% yield; mp: 94°C; ^{1}H NMR (600 MHz, DMSO-d_6) δ 11.84 (s, 1H), 8.44 (s, 1H), 7.91 (d, J = 8.3 Hz, 2H), 7.78 (s, 1H), 7.68 (s, 1H), 7.49 (d, J = 4.3 Hz, 2H), 7.06 (d, J = 8.3 Hz, 2H), 5.47–5.42 (m, 1H), 5.11–5.05 (m, 1H), 4.65 (d, J = 6.5 Hz, 2H), 2.10 (d, J = 7.9 Hz, 2H), 2.06 (d, J = 6.9 Hz, 2H), 1.73 (s, 3H), 1.63 (s, 3H), 1.58 (s, 3H). ^{13}C NMR (151 MHz, DMSO-d_6) δ 163.11, 161.82, 145.85, 141.19, 137.24, 134.13, 131.51, 131.20, 130.00, 126.62, 126.18, 125.60, 125.59, 124.22, 119.78, 114.85, 65.14, 39.39, 26.28, 25.92, 18.03, 16.86. HRMS-APCI *m/z* calcd for $C_{24}H_{28}ClN_2O_2$ $[M+H]^+$, 411.1834, found 411.1839.

(*E*)-*N*′-(4-Chlorobenzylidene)-4-{[(*E*)-3,7-dimethylocta-2,6-dien-1-yl]oxy}benzohydrazide (**8**): White solid; 27.6% yield; mp: 131–132°C; ^{1}H NMR (600 MHz, Acetone-d_6) δ 11.01 (s, 1H), 8.50 (s, 1H), 7.98 (d, J = 9.5 Hz, 2H), 7.77 (s, 1H), 7.56 (s, 1H), 7.48 (d, J = 6.5 Hz, 2H), 7.04 (d, J = 9.5 Hz, 2H), 5.54–5.48 (m, 1H), 5.17–5.11 (m, 1H), 4.69 (d, J = 6.1 Hz, 2H), 2.14 (d, J = 29.3 Hz, 2H), 2.07 (d, J = 2.3 Hz, 2H), 1.79 (s, 3H), 1.67 (s, 3H), 1.62 (s, 3H). ^{13}C NMR (151 MHz, Acetone-d_6) δ 161.87, 160.58, 140.77, 136.62, 134.94, 133.94, 133.15, 131.24, 129.96, 129.03, 128.82, 128.55, 125.72, 123.82, 119.62, 114.33, 64.86, 39.26, 26.15, 24.91, 16.84, 15.80. HRMS-APCI *m/z* calcd for $C_{24}H_{28}ClN_2O_2$ $[M+H]^+$, 411.1834, found 411.1837.

(*E*)-*N*′-(3-Bromobenzylidene)-4-{[(*E*)-3,7-dimethylocta-2,6-dien-1-yl]oxy}benzohydrazide (**9**): Off-white solid; 16.9% yield; mp: 98–101°C; ^{1}H NMR (600 MHz, DMSO-d_6) δ 11.83 (s, 1H), 8.05 (s, 3H), 7.94 (d, J = 7.8 Hz, 3H), 7.86–7.82 (m, 3H), 7.49 (d, J = 2.5 Hz, 2H), 7.03–6.95 (m, 1H), 5.46–5.42 (m, 1H), 5.09–5.06 (m, 1H), 4.63 (d, J = 10.8 Hz, 1H), 2.09 (d, J = 6.6 Hz, 1H), 2.05 (d, J = 7.7 Hz, 1H), 1.72 (s, 3H), 1.64 (s, 3H), 1.58 (s, 3H). ^{13}C NMR (151 MHz, DMSO-d_6) δ 166.44, 141.19, 135.98, 134.14, 132.20, 131.35, 128.73, 124.22, 122.16, 116.68, 40.57 (all carbons could not be accounted for due to poor solubility). HRMS-APCI *m/z* calcd for $C_{24}H_{28}BrN_2O_2$ $[M+H]^+$, 455.1329, found 455.1363.

(*E*)-*N*′-(4-Bromobenzylidene)-4-{[(*E*)-3,7-dimethylocta-2,6-dien-1-yl]oxy}benzohydrazide (**10**): Off-white solid; 34.2% yield; mp: 138–139°C; ^{1}H NMR (600 MHz, Acetone-d_6) δ 10.99 (s, 1H), 8.48 (s, 1H), 7.99–7.95 (m, 2H), 7.89–7.86 (m, 2H), 7.71 (d, J = 8.4 Hz, 1H), 7.63 (d, J = 8.8 Hz, 1H), 7.07–7.02 (m, 2H), 5.53–5.48 (m, 1H), 5.16–5.10 (m, 1H), 4.69 (d, J = 6.3 Hz, 2H), 2.16 (d, J = 7.3 Hz, 2H), 2.06 (d, J = 3.7 Hz, 2H), 1.79 (s, 3H), 1.67 (s, 3H), 1.62 (s, 3H). ^{13}C NMR (151 MHz, Acetone-d_6) δ 161.88, 160.71, 145.47, 140.76, 134.34, 132.04, 131.81, 131.24, 130.14, 129.41, 128.78, 125.71, 123.81, 123.25, 119.62, 114.34, 64.86, 39.26, 26.15, 24.91, 16.83, 15.79. HRMS-APCI *m/z* calcd for $C_{24}H_{28}BrN_2O_2$ $[M+H]^+$, 455.1329, found 455.1343.

(*E*)-*N*′-(2,5-Dimethoxybenzylidene)-4-{[(*E*)-3,7-dimethylocta-2,6-dien-1-yl]oxy}benzohydrazide (**11**): Light yellow solid; 62.1% yield; mp: 140.5–141.8°C; ^{1}H NMR (600 MHz, DMSO-d_6) δ 11.72 (s, 1H), 8.78 (s, 1H), 7.91 (d, J = 8.4 Hz, 2H), 7.39 (s, 1H), 7.08 (s, 1H), 7.06-7.00 (m, 3H), 5.47–5.42 (m, 1H), 5.11–5.05 (m, 1H), 4.64 (d, J = 6.5 Hz, 2H), 3.83 (s, 3H), 3.77 (s, 3H), 2.09 (d, J = 6.7 Hz, 2H), 2.06 (d, J = 7.0 Hz, 2H), 1.73 (s, 3H), 1.64 (s, 3H), 1.58 (s, 3H). ^{13}C NMR (151 MHz, DMSO-d_6) δ 162.84, 161.70, 153.77, 152.72, 142.93, 141.15, 131.51, 129.91, 125.75, 124.22, 123.64, 119.81, 117.89, 114.81, 113.92, 109.73, 65.12, 56.74, 55.95, 39.39, 26.28, 25.92, 18.03, 16.85. HRMS-APCI *m/z* calcd for $C_{26}H_{33}N_2O_4$ $[M+H]^+$, 437.2435, found 437.2459.

(*E*)-*N*′-(3,4-Dimethoxybenzylidene)-4-{[(*E*)-3,7-dimethylocta-2,6-dien-1-yl]oxy}benzohydrazide (**12**): Off-white solid; 50.8% yield; mp: 140–142°C; ^{1}H NMR (600 MHz, DMSO-d_6) δ 11.59 (s, 1H), 8.38 (s, 1H), 7.89 (d, J = 8.3 Hz, 2H), 7.34 (s, 1H), 7.20 (d, J = 8.2 Hz, 1H), 7.04 (t, J = 9.8 Hz, 3H), 5.47–5.42 (m, 1H), 5.08 (t, J = 6.9 Hz, 1H), 4.64 (d, J = 6.5 Hz, 2H), 3.82 (s, 3H), 3.32 (s, 3H), 2.09 (d, J = 7.1 Hz, 2H), 2.06 (d, J = 7.1 Hz, 2H), 1.73 (s, 3H), 1.64 (s, 3H), 1.58 (s, 3H). ^{13}C NMR (151 MHz, DMSO-d_6) δ 162.86, 161.62, 151.15, 149.58, 147.87, 141.14, 131.51, 129.85, 127.72, 125.97, 124.22, 122.16, 119.82, 114.82, 112.05, 108.83, 65.12, 56.07, 55.96, 39.39, 26.28, 25.92, 18.03, 16.86. HRMS-APCI *m/z* calcd for $C_{26}H_{33}N_2O_4$ $[M+H]^+$, 437.2561, found 437.2542.

(*E*)-*N*′-(3,4-Dichlorobenzylidene)-4-{[(*E*)-3,7-dimethylocta-2,6-dien-1-yl]oxy}benzohydrazide (**13**): White solid; 37.8% yield; mp: 119–120°C; ^{1}H NMR (600 MHz, Acetone-d_6) δ 11.14 (s, 1H), 8.48 (s, 1H), 7.98 (dd, J = 8.7, 1.3 Hz, 2H), 7.93 (s, 1H), 7.72 (d, J = 8.4 Hz, 1H), 7.63 (dd, J = 8.3, 1.1 Hz, 1H), 7.05 (dd, J = 8.8, 1.2 Hz, 2H), 5.53–5.48 (m, 1H), 5.16–5.10 (m, 1H), 4.69 (d, J = 6.4 Hz, 2H), 2.14 (d, J =;20.5 Hz, 2H), 2.09 (d, J = 21.8 Hz, 2H), 1.79 (s, 3H), 1.67 (s, 3H), 1.62 (s, 3H). ^{13}C NMR (151 MHz, Acetone-d_6) δ 161.98, 161.97, 144.22, 140.79, 135.78, 132.70, 132.35, 131.24, 130.89, 129.51, 128.47, 126.71, 125.50, 123.81, 119.59, 114.37, 64.87, 39.26, 26.15, 24.91, 16.84, 15.80. HRMS-APCI *m/z* calcd for $C_{24}H_{27}Cl_2N_2O_2$ $[M+H]^+$, 445.1444, found 445.1470.

15214184, 2024, 10, Downloaded from https://onlinelibrary.wiley.com/doi/10.1002/ardp.202400430 by North-West University, Wiley Online Library on [05/01/2026]. See the Terms and Conditions (https://onlinelibrary.wiley.com/terms-and-conditions) on Wiley Online Library for rules of use; OA articles are governed by the applicable Creative Commons License

(*E*)-4-{[(*E*)-3,7-Dimethylocta-2,6-dien-1-yl]oxy}-*N*′-(3-methoxybenzylidene)benzohydrazide (**14**): White solid; 39.9% yield; mp: 96. °C; ^{1}H NMR (600 MHz, DMSO-d_6) δ 11.71 (s, 1H), 8.44 (s, 1H), 7.93–7.88 (m, 2H), 7.41–7.35 (m, 1H), 7.28 (s, 2H), 7.08–6.99 (m, 3H), 5.48–5.42 (m, 1H), 5.11–5.05 (m, 1H), 4.64 (d, J = 3.1 Hz, 2H), 3.82 (s, 3H), 2.09 (d, J = 6.4 Hz, 2H), 2.06 (d, J = 6.4 Hz, 2H), 1.73 (s, 3H), 1.64 (s, 3H), 1.58 (s, 3H). ^{13}C NMR (151 MHz, DMSO-d_6) δ 162.74, 161.72, 160.05, 147.53, 141.17, 136.42, 131.51, 130.40, 129.95, 125.78, 124.23, 120.41, 119.80, 116.52, 114.84, 111.68, 65.14, 55.65, 40.58, 26.28, 25.92, 18.03, 16.86. HRMS-APCI *m/z* calcd for $C_{25}H_{31}N_2O_3$ $[M+H]^+$, 407.2329, found 407.2359.

(*E*)-4-{[(*E*)-3,7-Dimethylocta-2,6-dien-1-yl]oxy}-*N*′-(2-methylbenzylidene)benzohydrazide (**15**): White solid; 26% yield; mp: 105°C; ^{1}H NMR (600 MHz, Acetone-d_6) δ 10.96 (s, 1H), 8.80 (s, 1H), 7.99 (d, J = 8.3 Hz, 2H), 7.95–7.90 (m,1H), 7.33–7.21 (m, 3H), 7.07–7.02 (m, 2H), 5.53–5.48 (m, 1H), 5.16–5.11 (m, 1H), 4.69 (d, J = 6.4 Hz, 2H), 2.48 (s, 3H), 2.16 (d, J = 0.8 Hz, 2H), 2.12 (d, J = 3.2 Hz, 2H), 1.79 (s, 3H), 1.67 (s, 3H), 1.62 (s, 3H). ^{13}C NMR (151 MHz, Acetone-d_6) δ 161.80, 161.78, 145.40, 140.73, 136.89, 132.87, 131.24, 130.75, 129.46, 126.35, 126.33, 126.05, 125.89, 123.82, 119.65, 114.32, 64.85, 39.26, 26.15, 24.91, 18.70, 16.84, 15.79. HRMS-APCI *m/z* calcd for $C_{25}H_{31}N_2O_2$ $[M+H]^+$, 391.2380, found 391.2398.

4.2 | Biological assays

In each assay, cell or parasite growth was compared with two control groups: the untreated control wells (exhibiting 100% cell growth) and the medium control wells (exhibiting 0% cell growth).

The findings were presented as a percentage decrease in cell or parasite viability relative to the control wells, and an IC_{50} value was determined.

4.2.1 | In vitro antitrypanosomal assay

The assay for the anti-*Trypanosoma* activity was as described in earlier literature.[51] The ß-galactosidase expressing Tulahuen CL_2 strain and MRC-5_{SV2} (human foetal lung fibroblast cells) host cells were used in the in vitro *T. cruzi* assay. 4×10^3 MRC-5_{sv2} cells were infected with 4×10^4 parasites per well. After 4 h of infection, the diluted compounds were added to the infected cells. Following a 7-day incubation period at 37°C, chlorophenol red ß-D-galactopranoside (CPRG) was added, and the parasite burden was assessed spectrophotometrically by measuring the colour change at 540 nm.

The resazurin assay was used to quantify the drug activity against *T. brucei* and *T. b. rhodesiense*. *T. brucei* Squib 427 was cultured at 1.5×10^4 parasites per well, and *T. b. rhodesiense* STIB-900 was cultured at 4×10^3 parasites per well. After an incubation period of 3 days, resazurin was added. After adding resazurin, there is another incubation period of 24 h (*T. brucei*) and 6 h (*T. b. rhodesiense*). After these additional incubation periods, the impact of the compounds on parasite viability was quantified by fluorescence detection (λ_{ex} 550 nm, λ_{em} 590 nm).

4.2.2 | In vitro antileishmanial assay

The anti-*Leishmania* activity was determined as described elsewhere.[51] Primary peritoneal mouse macrophages (PMM) were used as host cells. These PMM were infected with 4.5×10^5 parasites per well of 3×10^4 PMM. Following 2 h of infection, dilutions of the compounds were added to the infected cells. The cells were incubated for 5 days, and the parasite burden was assessed using staining with a 10% Giesma solution and evaluated by microscopy. The parasite burden was determined as the mean number of amastigotes per macrophage.

4.2.3 | In vitro cytotoxicity assay

The evaluation of cytotoxicity against MRC-5_{sv2} cells was performed as previously described.[51] A concentration of 1.5×10^5 MRC-5_{sv2} cells per millilitre was incubated with the compound dilutions at 37°C and 5% CO_2. Cell viability was evaluated by using a fluorescence-based assay after a 3-day incubation period, following the addition of 50 µL of resazurin per well. After incubation for 4 h at 37°C, fluorescence (λ_{ex} 550 nm, λ_{em} 590 nm) was measured.

ACKNOWLEDGEMENTS

The authors wish to acknowledge Natascha Van Pelt, An Matheeussen, Pim-Bart Feijens and Matthias Sempels for their contribution to performing the antiparasitic assays. R.M.B. and G.C. participate in COST Action Onehealthdrugs. LMPH is a partner of the Excellence Centre 'Infla-Med' (www.uantwerpen.be/infla-med). This project is funded by the South African Medical Research Council (SAMRC), through the "Self-Initiated Research (MRC-SIR)" Grant awarded to RMB. Dr Daniel Otto and Dr Johan Jordaan from the SASOL Centre of Chemistry at North-West University conducted the recording of NMR and HRMS spectra.

CONFLICTS OF INTEREST STATEMENT

The authors declare no conflicts of interest.

DATA AVAILABILITY STATEMENT

The supplementary material includes ^{1}H and ^{13}C NMR spectra and HRMS spectra of the compounds documented in this work.

REFERENCES

[1] A. Abera, T. Mamecha, E. Abose, B. Bokicho, A. Ashole, T. Bishaw, A. Mariyo, B. Bogale, H. Terefe, H Tadesse, M. Belachew, H. Difabachew, A. Eukubay, S. Kinde, A. Ali, F. Regasa, F. Seife, Z. Kebede, M. Wossen, G. Tollera, M. Hailu, N. Manaye, N. Van Reet, G. Priotto, J. van Griensven, M. Pareyn, G. Tasew, *Emerging Infect. Dis.* **2024**, *30*(1), 125. https://doi.org/10.3201/eid3001.231319

[2] E. A. Dickie, F. Giordani, M. K. Gould, P. Mäser, C. Burri, J. C. Mottram, S. P. S. Rao, M. P. Barrett, *Trop. Med. Infect. Dis.* **2020**, *5*, 29. https://doi.org/10.3390/tropicalmed5010029

15214184, 2024, 10, Downloaded from https://onlinelibrary.wiley.com/doi/10.1002/ardp.202400430 by North-West University, Wiley Online Library on [05/01/2026]. See the Terms and Conditions (https://onlinelibrary.wiley.com/terms-and-conditions) on Wiley Online Library for rules of use; OA articles are governed by the applicable Creative Commons License

[3] D. Steverding, *Parasit. Vectors* **2008**, *1*(1), 1. https://doi.org/10.1186/1756-3305-1-3

[4] Trypanosomiasis, human African (sleeping sickness). https://www.who.int/news-room/fact-sheets/detail/trypanosomiasis-human-african-(sleeping-sickness) (accessed: March 2024).

[5] E. Pays, M. Radwanska, S. Magez, *Annu. Rev. Pathol. Mech. Dis.* **2023**, *18*, 19. https://doi.org/10.1146/annurev-pathmechdis-031621-025153

[6] S. J. Migchelsen, P. Büscher, A. I. M. Hoepelman, H. D. F. H. Schallig, E. R. Adams, *Int. J. Infect. Dis.* **2011**, *15*, e517. https://doi.org/10.1016/j.ijid.2011.03.018

[7] Y. Ortiz-Martínez, M. G. Kouamé, F. Bongomin, S. Lakoh, A. F. Henao-Martínez, *Curr. Trop. Med. Rep.* **2023**, *10*(4), 222. https://doi.org/10.1007/s40475-023-00304-w

[8] R. Idro, R. Ogwang, A. Barragan, J. V. Raimondo, W. Masocha, *Front. Immunol.* **2022**, *13*, 791488. https://doi.org/10.3389/fimmu.2022.791488

[9] WHO interim guidelines for the treatment of gambiense human African trypanosomiasis. https://iris.who.int/bitstream/handle/10665/326178/9789241550567-eng.pdf (accessed: March 2024).

[10] V. K. Betu Kumeso, W. M. Kalonji, S. Rembry, O. Valverde Mordt, D. Ngolo Tete, A. Prêtre, S. Delhomme, M. Ilunga Wa Kyhi, M. Camara, J. Catusse, S. Schneitter, M. Nusbaumer, E. Mwamba Miaka, H. Mahenzi Mbembo, J. Makaya Mayawula, M. Layba Camara, F. Akwaso Massa, L. Kaninda Badibabi, A. Kasongo Bonama, P. Kavunga Lukula, S. Mutanda Kalonji, P. Mariero Philemon, R. Mokilifi Nganyonyi, H. Embana Mankiara, A. Asuka Akongo Nguba, V. Kobo Muanza, E. Mulenge Nasandhel, A. Fifi Nzeza Bambuwu, B. Scherrer, N. Strub-Wourgaft, A. Tarral, *Lancet Infect. Dis.* **2023**, *23*(4), 463. https://doi.org/10.1016/S1473-3099(22)00660-0

[11] Chagas disease (also known as American trypanosomiasis). https://www.who.int/news-room/fact-sheets/detail/chagas-disease-(american-trypanosomiasis) (accessed: March 2024).

[12] A. F. Francisco, S. Jayawardhana, F. Olmo, M. D. Lewis, S. R. Wilkinson, M. C. Taylor, J. M. Kelly, *Molecules* **2020**, *25*, 2799. https://doi.org/10.3390/molecules25122799

[13] S. Pathak, M. Bhardwaj, N. Agrawal, A. Bhardwaj, *Chem. Biol. Drug Des.* **2023**, *102*(3), 587. https://doi.org/10.1111/cbdd.14257

[14] J. A. Castro, M. M. de Mecca, L. C. Bartel, *Hum. Exp. Toxicol.* **2006**, *25*(8), 471.

[15] L. Gradoni, R. López-Vélez, M. Mokni. Manual on case management and surveillance of the leishmaniases in the WHO European region. https://iris.who.int/bitstream/handle/10665/344118/9789289052511-eng.pdf?sequence=1&isAllowed=y (accessed: March 2024).

[16] G. Michel, C. Pomares, B. Ferrua, P. Marty, *Acta Trop.* **2011**, *119*(2-3), 69. https://doi.org/10.1016/j.actatropica.2011.05.012

[17] C. Maia, C. Conceição, A. Pereira, R. Rocha, M. Ortuño, C. Muñoz, Z. Jumakanova, P. Pérez-Cutillas, Y. Özbel, S. Töz, G. Baneth, B. Monge-Maillo, E. Gasimov, Y. Van der Stede, G. Torres, C. M. Gossner, E. Berriatua, *PLoS Neglected Trop. Dis.* **2023**, *17*(7), e0011497. https://doi.org/10.1371/journal.pntd.0011497

[18] A. Datta, I. Podder, A. Das, A. Sil, N. Das, *Indian J. Dermatol.* **2021**, *66*(1), 34. https://doi.org/10.4103/ijd.ijd_264_20

[19] S. Saurabh, M. Mahabir, *Trop. Doct.* **2020**, *50*(1), 37. https://doi.org/10.1177/0049475519877317

[20] J. van Griensven, T. P. Dorlo, E. Diro, C. Costa, S. Burza, *Lancet Infect. Dis.* **2024**, *24*(1), e36. https://doi.org/10.1016/S1473-3099(23)00353-5

[21] M. De Rycker, S. Wyllie, D. Horn, K. D. Read, I. H. Gilbert, *Nat. Rev. Microbiol.* **2023**, *21*(1), 35. https://doi.org/10.1038/s41579-022-00777-y

[22] S. Moser, H. Pichler, *Appl. Microbiol. Biotechnol.* **2019**, *103*, 5501. https://doi.org/10.1007/s00253-019-09892-y

[23] F. Bouvier, A. Rahier, B. Camara, *Prog. Lipid Res.* **2005**, *44*, 357. https://doi.org/10.1016/j.plipres.2005.09.003

[24] M. Zielińska-Błajet, J. Feder-Kubis, *Int. J. Mol. Sci.* **2020**, *21*(19), 7078. https://doi.org/10.3390/ijms21197078

[25] M. H. P. Lira, F. P. Andrade Júnior, G. F. Q. Moraes, G. S. Macena, F. O. Pereira, I. O. Lima, *J. Essent. Oil Res.* **2020**, *32*(3), 187. https://doi.org/10.1080/10412905.2020.1745697

[26] D. P. de Sousa, R. O. S. Damasceno, R. Amorati, H. A. Elshabrawy, R. D. de Castro, D. P. Bezerra, V. R. V. Nunes, R. C. Gomes, T. C. Lima, *Biomolecules* **2023**, *13*(7), 1144. https://doi.org/10.3390/biom13071144

[27] L. C. R. F. Lins, I. M. A. Santos, M. S. de Melo, P. dos Passos Menezes, A. A. Saraújo, R. de Souza Nunes, M. R. V. Dos Santos, I. A. de Medeiros, E. A. N. Ribeiro, J. R. dos Santos, M. Matchioro, *Bol. Latinoam. Caribe Plantas Med. Aromat.* **2014**, *13*(6), 557.

[28] K. R. Rekha, G. P. Selvakumar, S. Sethupathy, K. Santha, R. I. Sivakamasundari, *J. Mol. Neurosci.* **2013**, *51*(3), 851. https://doi.org/10.1007/s12031-013-0074-9

[29] D. N. Roy, *Terpenoids against human diseases*, CRC Press, Taylor and Francis Group, Boca Raton **2019**, https://doi.org/10.1201/9781351026703

[30] S. Inouye, T. Takizawa, H. Yamaguchi, *J. Antimicrob. Chemother.* **2001**, *47*(5), 565.

[31] R. L. van Zyl, S. T. Seatlholo, S. F. van Vuuren, A. M. Viljoen, *J. Essent. Oil Res.* **2006**, *18*, 129. https://doi.org/10.1080/10412905.2006.12067134

[32] G. S. Silva, J. N. J. Marques, E. P. M. Linhares, C. M. Bonora, É. T. Costa, M. F. Saraiva, *Chem. Biol. Interact.* **2022**, *362*, 109994. https://doi.org/10.1016/j.cbi.2022.109994

[33] S. Babukumar, V. Vinothkumar, C. Sankaranarayanan, S. Srinivasan, *Pharm. Biol.* **2017**, *55*(1), 1442. https://doi.org/10.1080/13880209.2017.1301494

[34] M. I. Chavez, M. Soto, F. A. Cimino, A. F. Olea, L. Espinoza, K. Díaz, L. Taborga, *Int. J. Mol. Sci.* **2018**, *19*, 1601. https://doi.org/10.3390/ijms19061601

[35] G. F. Makhaeva, N. A. Elkina, E. V. Shchegolkov, N. P. Boltneva, S. V. Lushchekina, O. G. Serebryakova, E. V. Rudakova, N. V. Kovaleva, E. V. Radchenko, V. A. Palyulin, Y. V. Burgart, V. I. Saloutin, S. O. Bachurin, R. J. Richardson, *Bioorg. Chem.* **2019**, *91*, 103097. https://doi.org/10.1016/j.bioorg.2019.103097

[36] J. V. Ragavendran, D. Sriram, S. K. Patel, I. V. Reddy, N. Bharathwajan, J. Stables, P. Yogeeswari, *Eur. J. Med. Chem.* **2007**, *42*, 146. https://doi.org/10.1016/j.ejmech.2006.08.010

[37] N. Ergenç, N. S. Günay, R. Demirdamar, *Eur. J. Med. Chem.* **1998**, *33*(2), 143. https://doi.org/10.1016/S0223-5234(98)80039-1

[38] A. R. Todeschini, A. L. P. de Miranda, K. C. M. da Silva, S. C. Parrini, E. J. Barreiro, *Eur. J. Med. Chem.* **1998**, *33*(3), 189. https://doi.org/10.1016/S0223-5234(98)80008-1

[39] P. Vicini, F. Zani, P. Cozzini, I. Doytchinova, *Eur. J. Med. Chem.* **2002**, *37*(7), 553. https://doi.org/10.1016/S0223-5234(02)01378-8

[40] Ş. G. Küçükgüzel, E. E. Oruç, S. Rollas, F. Şahin, A. Özbek, *Eur. J. Med. Chem.* **2002**, *37*(3), 197. https://doi.org/10.1016/S0223-5234(01)01326-5

[41] A. H. Abadi, A. A. H. Eissa, G. S. Hassan, *Chem. Pharm. Bull.* **2003**, *51*(7), 838. https://doi.org/10.1248/cpb.51.838

[42] A. G. Silva, G. Zapata-Sudo, A. E. Kummerle, C. A. Fraga, E. J. Barreiro, R. T. Sudo, *Bioorg. Med. Chem.* **2005**, *13*(10), 3431. https://doi.org/10.1016/j.bmc.2005.03.003

[43] L. Camaioni, D. Lambert, B. Sendid, M. Billamboz, S. Jawhara, *Antibiotics* **2023**, *12*(6), 10. https://doi.org/10.3390/antibiotics12061043

[44] M. T. Abdel-Aal, W. A. El-Sayed, E.-S. H. El-Ashry, *Arch. Pharm.* **2006**, *339*(12), 656. https://doi.org/10.1002/ardp.200600100

[45] A. Bernardino, A. Gomes, K. Charret, A. Freitas, G. Machado, M. Canto-Cavalheiro, L. Leon, V. Amaral, *Eur. J. Med. Chem.* **2006**, *41*(1), 80. https://doi.org/10.1016/j.ejmech.2005.10.007

15214184, 2024, 10, Downloaded from https://onlinelibrary.wiley.com/doi/10.1002/ardp.202400430 by North-West University, Wiley Online Library on [05/01/2026]. See the Terms and Conditions (https://onlinelibrary.wiley.com/terms-and-conditions) on Wiley Online Library for rules of use; OA articles are governed by the applicable Creative Commons License

[46] Ł. Popiołek, *Med. Chem. Res.* **2017**, *26*, 287. https://doi.org/10.1007/s00044-016-1756-y

[47] M. Abidov, *Health Promo. Phys. Act.* **2017**, *2*(3), 9. https://doi.org/10.5604/01.3001.0010.7718

[48] K. A. Chirwa, K. R. Francisco, P. S. Dube, H. Park, L. J. Legoabe, T. R. Teixeira, C. R. Caffrey, R. M. Beteck, *ChemMedChem* **2024**, *19*(9), e202300667. https://doi.org/10.1002/cmdc.202300667

[49] S. Hoet, C. Stevigny, M.-F. Herent, J. l Quetin-Leclercq, *Planta Med.* **2006**, *72*, 480. https://doi.org/10.1055/s-2005-916255

[50] R. Essid, F. Z. Rahali, K. Msaada, I. Sghair, M. Hammami, A. Bouratbine, K. Aoun, F. Limam, *Ind. Crops Prod.* **2015**, *77*, 795. https://doi.org/10.1016/j.indcrop.2015.09.049

[51] C. B. Hartman, P. S. Dube, L. J. Legoabe, N. Van Pelt, A. Matheeussen, G. Caljon, R. M. Beteck, *Arch. Pharm.* **2024**, *357*(6), e2300319. https://doi.org/10.1002/ardp.202300319

SUPPORTING INFORMATION

Additional supporting information can be found online in the Supporting Information section at the end of this article.

How to cite this article: J. Jooste, L. J. Legoabe, K. Ilbeigi, G. Caljon, R. M. Beteck, *Arch. Pharm.* **2024**;*357*:e2400430. https://doi.org/10.1002/ardp.202400430

15214184, 2024, 10, Downloaded from https://onlinelibrary.wiley.com/doi/10.1002/ardp.202400430 by North-West University, Wiley Online Library on [05/01/2026]. See the Terms and Conditions (https://onlinelibrary.wiley.com/terms-and-conditions) on Wiley Online Library for rules of use; OA articles are governed by the applicable Creative Commons License